Available online at www.sciencedirect.com
SCIENCE DIRECT®
Journal of Magnetic Resonance 174 (2005) 68–77
JMR Journal of Magnetic Resonance
www.elsevier.com/locate/jmr

Cumulative "roof effect" in high-resolution in vivo ^{31}P NMR spectra of human calf muscle and the Clebsch–Gordan coefficients of ATP at 1.5 T

Leif Schröder [a,*], Christian Schmitz [b], Peter Bachert [a,*]

[a] *Abteilung Medizinische Physik in der Radiologie, Deutsches Krebsforschungszentrum (dkfz), D-69120 Heidelberg, Germany*
[b] *Biophysikalische Chemie, Institut für Physikalische Chemie, Universität Heidelberg, D-69120 Heidelberg, Germany*

Received 18 August 2004; revised 18 January 2005

Abstract

NMR spectra of non-weakly coupled spin systems exhibit asymmetries in line intensities known as "roof effect" in 1D spectroscopy. Due to limited spectral resolution, this effect has not been paid much attention so far in in vivo spectroscopy. But when high-quality spectra are obtained, this effect should be taken into account to explain the quantum-mechanical fine structure of the system. Adenosine 5′-triphosphate (ATP) represents a ^{31}P spin system with multiple line splittings which are caused by *J*-couplings of medium strength at 1.5 T. We analyzed the ATP roof effect in vivo, especially for the β-ATP multiplet. The intensities of its outer resonances deviate by ca. 12.5% from a symmetrical triplet. As this asymmetry reflects the transition from Paschen–Back to Zeeman effect with total spin that is largely broken up, the Clebsch–Gordan coefficients of the system can be indicated in analogy to the hyperfine structure of hydrogen. Taking the roof effect into account, the χ^2 of fitting in vivo ATP resonances is reduced by ca. 9% ($p < 0.005$).

Keywords: ^{31}P NMR; ATP; State mixing; Roof effect; Human calf muscle

1. Introduction

The ^{31}P NMR resonances of adenosine 5′-triphosphate (ATP) are multiplets which can be resolved in vivo at 1.5 T, in particular, in spectra of human muscle tissue. Because of the constant signal intensity, they are often used as internal reference for relative quantification of the concentrations of other phosphorus metabolites. Details of the seven resonances detectable at 1.5 T should be taken into account for accurate fitting whenever high resolution is achieved, e.g., in skeletal muscle.

A quantum-mechanical effect which was—to our knowledge—not considered so far in NMR spectroscopy of this important biomolecule is the so-called "roof effect": because of partially suppressed transitions between singlet and triplet states during the transition from weakly coupled AX systems to strongly coupled AB systems, relative intensities of multiplet components change.

A tissue metabolite which shows this effect clearly in the ^{1}H NMR spectrum at 1.5 T is citrate (Cit) [1]. The difference in chemical shifts of the coupled spins, $\Delta\nu$, is small compared to the scalar coupling constant *J* (ratio ca. 1:2 at 1.5 T). Therefore, deviations from the Paschen–Back effect (both spins are coupled separately to the external field) which is normally valid under these experimental conditions occur and cause a strong attenuation of the outer resonances, while the inner ones are amplified by the same amount.

* Corresponding authors. Fax: +49 6221 422531 (P. Bachert).
E-mail address: p.bachert@dkfz-heidelberg.de (P. Bachert).
URL: www.dkfz.de/mrspek (P. Bachert).

1090-7807/$ - see front matter © 2005 Elsevier Inc. All rights reserved.
doi:10.1016/j.jmr.2005.01.011

The effect is less pronounced for the three ^{31}P nuclei in ATP, but precise data processing should take into account that also in this system spectra are not first order. The purpose of this contribution is to quantify this effect in vivo. Particularly, the β-ATP resonance is a doublet-of-doublets and the resulting roof effect arising from the contributions of two interactions could be studied in detail. Furthermore, the impact of pH variation and chelation of Mg^{2+} ions by the triphosphate chain on the roof effect—two processes which affect in vivo ^{31}P NMR spectra—was studied in model solutions in order to estimate a possible variance in spectra from living tissue.

2. Theory

We consider a scalar-coupled system of two spin-$\frac{1}{2}$ nuclei in an external field. The appropriate eigenbase in the case of non-weak coupling is obtained by a rotation with angle ϑ of a two-dimensional subspace of the four-dimensional Hilbert space spanned by the product states of a weakly coupled two-spin system [2]. The rotation matrix **U** contains the coefficients $+\cos\vartheta$ and $\pm\sin\vartheta$. According to [3] we use the convention of a negative mixing angle for scalar coupling. Hence, the coupling constant J and chemical-shift difference $\Delta\nu$ are connected with ϑ via

$$\tan 2\vartheta = -\frac{J}{\Delta\nu}, \tag{1}$$

(the ratio is also known as perturbation parameter). The sin/cos functions correspond to Clebsch–Gordan coefficients (CGCs) known from the hydrogen hyperfine structure and characterize the system for a specific field strength; in particular, the intensities of single-quantum transitions of the two-spin system depend on ϑ. An increase of the coupling strength ($\vartheta \to -45°$) causes suppression of the transitions where the singlet state is involved and amplification of the transitions within the triplet. Since this state originates from the second-lowest product state ($|{+}{-}\rangle$), the outer resonances are affected (i.e., resonances a and d, if the four signals are denoted a...d with decreasing frequency according to [3]).

The relation between ϑ and the line intensities is well known [4] and reads

$$I_1 \propto 1 - \sin 2\vartheta \quad \text{transitions b and c}, \tag{2}$$

$$I_2 \propto 1 + \sin 2\vartheta \quad \text{transitions a and d}. \tag{3}$$

These quantities can be directly applied for the γ- and α-ATP doublets. Abbreviating the $\sin 2\vartheta$ terms, the relative intensities of the doublets are (in the order of decreasing frequencies): $1-x$, $1+x$ for γ-ATP and $1-y$, $1+y$ for α-ATP. Because of the larger $\Delta\nu$ with the β nucleus, the effect is less pronounced for γ-ATP and $x \leqslant y$ if $J_{\alpha\beta} \approx J_{\gamma\beta}$. The total intensity $I_1 + I_2$ of each doublet remains constant.

The intensities of the β-ATP signals are obtained as follows (Fig. 1): the homonuclear scalar coupling constant $J_{\gamma\beta}$ causes two resonances with relative intensities $1+x$, $1-x$ which are further split by the α–β coupling ($J_{\alpha\beta}$). Each downfield resonance contributes with relative intensity $1+y$, the upfield signals with $1-y$. Because of the similar line splittings $J_{\gamma\beta} \approx J_{\alpha\beta}$, the two middle resonances of the doublet-of-doublets coincide at 1.5 T and only three signals can be resolved. Their intensities are calculated from the products of these intensities. Since the expected x and y are of the order of 10^{-2}, we neglect terms like $xy \propto 10^{-4}$ and obtain:

$$\begin{aligned} &1 : (1+x)(1+y) \approx 1 + x + y =: 1 + \Sigma, \\ &2 : (1+x)(1-y) + (1-x)(1+y) \approx 2, \\ &3 : (1-x)(1-y) \approx 1 - x - y =: 1 - \Sigma. \end{aligned} \tag{4}$$

The parameters x, y, and Σ now permit an appropriate fit of the ATP multiplets. Proper phase correction is crucial for detection of the roof effect, especially for the β-ATP multiplet at $\delta \approx -16$ ppm (relative to the phosphocreatine [PCr] resonance at $\delta = 0$ ppm).

Beside intensity changes non-weakly coupled spin systems also exhibit shifts of resonance frequencies as a consequence of transformation **U**. According to [4] the doublets are shifted apart so that the value of $\Delta\nu$ determined from the centers of the doublets is larger than the true one. Commonly, the chemical-shift difference is calculated using $\Delta\nu = \sqrt{|(\nu_a - \nu_d)(\nu_b - \nu_c)|}$ (e.g. [5]).

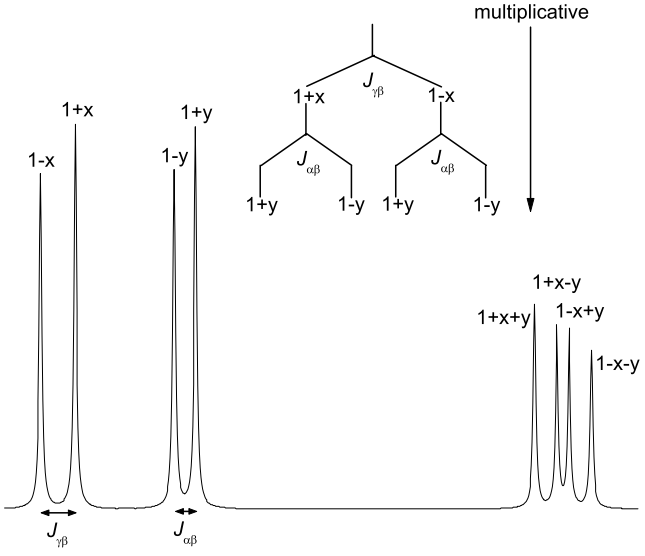

Fig. 1. Simulated spectrum of a three-spin system like that of ATP. The cumulative roof effect can be derived by the product of intensities after successive line splitting and then be approximated by the sum $\Sigma = x + y$ of the corrections of the doublets. If the doublet-of-doublets cannot be resolved completely, its central resonance has the constant relative intensity 2.

This procedure fails here because of the multiple splitting of the β-ATP signal. Hence, a direct relationship between the rotational angle ϑ and the line positions is needed. A similar problem was studied recently in the context of residual dipolar coupling of medium strength in in vivo ^{1}H NMR spectroscopy [6]. An asymmetry parameter A_P was defined which gives the energy corrections as a function of the mixing angle ϑ' of residual dipolar interactions (Sk is the coupling strength in energy units):

$$A_P(\vartheta') = Sk\left(\frac{\sin 2\vartheta'}{4} - \frac{\sin^2\vartheta'}{2\tan 2\vartheta'}\right). \quad (5)$$

In principle, the transformation $\mathbf{U} \neq \mathbb{1}$ is caused by the flip-flop operators $\hat{I}_+\hat{S}_-$ and $\hat{I}_-\hat{S}_+$ in the secular Hamiltonian of coupled spins. The only difference of scalar and dipolar coupling is the coefficients of these operators: -0.25 in the case of dipolar and $+0.5$ in the case of scalar interactions. As a consequence, the sign of the mixing angles is opposite ($\vartheta' > 0$), but all the resultant effects can be treated by analogy. Modification of Eq. (5) yields the parameter that determines the asymmetric line positions of scalar-coupled systems (h = Planck's constant, J in Hz):

$$A_P(\vartheta) = -Jh\left(\frac{\sin 2\vartheta}{2} - \frac{\sin^2\vartheta}{\tan 2\vartheta}\right). \quad (6)$$

In the case of the ATP spin system the condition at 1.5 T is expected to be very close to the regime of the Paschen–Back effect and the significance of $A_P(\vartheta)$ has to be verified.

$A_P(\vartheta)$ consists of two terms that originate from the Zeeman operator $\hat{H}_Z(\vartheta)$ and the operator $\hat{H}_J(\vartheta)$ of scalar coupling, respectively. The maximum shift of the line positions is $0.5 \times J$, while the ϑ-dependent variation of the intensities of the components is not limited and can account for changes of up to 100% (Eqs. (2) and (3)). Spin systems with small deviations from Paschen–Back effect, e.g., with $-5° < \vartheta < 0°$, are characterized by $J \ll \Delta\nu$. Hence, their chemical-shift difference $\Delta\nu$ varies insignificantly and can be derived in good approximation from the centers of the doublets.

In principle, A_P can be estimated directly from ϑ in the case of weak state mixing. The Taylor expansion of the function in Eq. (6) is

$$A_P(\vartheta) = -Jh\left(\frac{\pi}{360°}\vartheta + \frac{1}{6}\left(\frac{\pi}{180°}\vartheta\right)^3 + \frac{1}{15}\left(\frac{\pi}{180°}\vartheta\right)^5 + \mathcal{O}(\vartheta^7)\right). \quad (7)$$

Fig. 2 illustrates that the higher orders are important only for large $|\vartheta|$. For $0 \geqslant \vartheta \geqslant -15°$ the linear term suffices and since $\vartheta \geqslant -45°$, the expansion can be cut off after the cubic term for nearly the entire range of mixing angles. For weak mixing the shift (in Hz) of the multiplets is approximately $\pi J\vartheta/360°$.

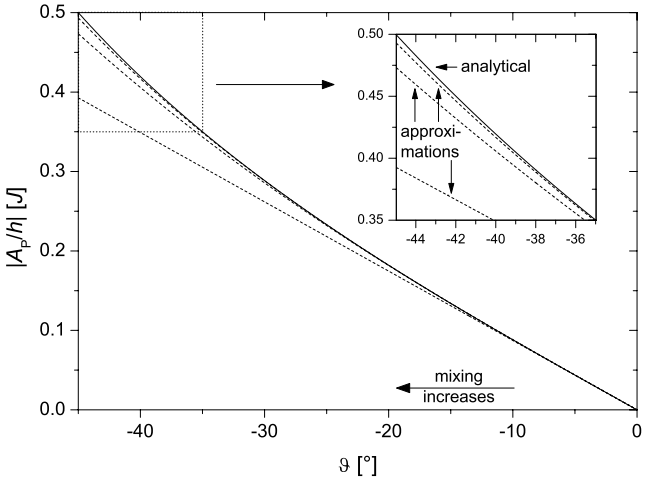

Fig. 2. Approximation of the asymmetry parameter A_P (Eq. (6); solid line) by Taylor expansion (Eq. (7); dashed lines). For weak state mixing, the linear approximation suffices to estimate quantum-mechanical corrections of the line positions. (Inset) Range of strong coupling with approximation of first, third, and fifth order.

The coupling constants are known from previous studies, e.g. [7], to be less than 20 Hz. Hence, the maximum shifts (corresponding to $B_0 \to 0$) are 10 Hz for the doublets and 20 Hz for the β-ATP multiplet (cumulative effect). Using 1.5-T data from [7], the minimum $\Delta\nu$ (derived from the multiplets' centers) is $\Delta\nu_{\alpha\beta} = 8.5$ ppm ≈ 219 Hz, while its maximum change owing to $A_P(\vartheta)$ would be $\Delta\nu'_{\alpha\beta} = (219 - 20 - 10)$ Hz $= 189$ Hz; this corresponds to a mixing angle $\vartheta = \frac{1}{2}\arctan(-\frac{20}{189}) \approx 3°$. Regarding the linear term in Eq. (7) the frequency shift is less than $8.73 \times 10^{-3} \times 20$ Hz $\times\, 3 \approx 0.5$ Hz for the doublets (i.e., 1 Hz for the β-ATP multiplet). These values do not exceed the spectral resolution in vivo and can therefore be neglected.

3. Materials and methods

3.1. Spectrometer

Phosphorus-31 NMR experiments were performed on a clinical whole-body MR scanner with field inductivity of 1.5 T (MAGNETOM Vision Plus with Helicon 2E magnet; Siemens AG, Erlangen, Germany).

A double resonant $\{^1\text{H}\}$–^{31}P surface coil (25×25 cm^2 "heart/liver coil"; Siemens) was used which consists of one linear-polarized receive/transmit coil (for excitation and detection at 63.6 MHz and excitation at 25.7 MHz) and one circular-polarized receive coil with integrated pre-amplifier (for detection of the ^{31}P signal). The antenna includes a high-pass filter for 63 MHz and a low-pass filter for 25 MHz to enable $\{^1\text{H}\}$–^{31}P spin decoupling.

3.2. In vivo NMR spectroscopy

Consent to the experiments according to procedures approved by the Institutional Review Board was obtained prior to each examination from informed healthy male volunteers ($n = 5$). Both calfs were placed symmetrically on the surface coil which was placed in the isocenter of the magnet horizontally on the patient table of the tomograph. First transverse MR images (300 mm field of view) were acquired, followed by slice-selective shim which yielded linewidths $\Delta\nu_{1/2}(^1\mathrm{H}) \approx 30-40$ Hz of the tissue water resonance.

Localized ^{31}P NMR spectra were obtained from a 8×8 two-dimensional spectroscopic imaging (SI) dataset (250 mm FOV, 50 mm thickness) with 8×8 phase-encoding steps, $NEX = 20$ acquisitions, and $TR = 1.1$ s (23.5 min measurement time). This repetition time was the minimum allowed according to safety guidelines that must be considered when the second RF channel is employed (SAR, recommended limit of RF power deposition for local exposition). A rectangular 2-ms pulse and the "decoupling" pulse train during the first 50 ms of the 256-ms acquisition period (a WALTZ-4 cycle with 2-ms pulses, interpulse delays of 0.5 ms), both at ^{1}H frequency, enabled NOE signal amplification owing to cross-polarization between dipolar-coupled ^{1}H-^{31}P spins [8,9] (in fact, there exists no scalar ^{1}H–^{31}P interaction for ATP which can be decoupled).

3.3. Model solutions and in vitro NMR spectroscopy

The chemical shifts of the resonances of the ATP polyphosphate chain depend on pH and on the concentration of Mg(II) ions [10]: they change monotonically when HCl or $MgCl_2$ is added to the solution. Moreover, chelation of Mg(II) ions causes a decrease of the J-coupling constants from ca. 19.5 to ca. 15.5 Hz on average [11]. Changes of $\Delta\nu$ and J affect the perturbation parameter and can therefore modify the roof effect.

To study and quantify these phenomena, we acquired spectra of ATP with and without Mg^{2+} ions (equimolar to ATP) using aqueous solutions of $MgCl_2 \cdot 6H_2O$ and ATP (45 mM). Each solution (200 ml in a cylindrical bottle of 60 mm diameter to cover a complete SI voxel) also contained PCr (90 mM) as internal chemical-shift reference ($\delta = 0$ ppm) and for frequency adjustment (all compounds purchased from Sigma–Aldrich, Steinheim, Germany). The selected range of pH ($4 \leqslant \mathrm{pH} \leqslant 8$, adjusted with 1 M HCl/1 M NaOH) leads to line positions which cover the full range of ^{31}P chemical shifts reported for this molecule [10].

All experiments were performed with the same antenna and pulse sequence as the in vivo measurements. Model solutions were placed in the center of the surface coil, flanked by two bottles containing 2 L water to obtain an adequate load of the coil. The slice-selective shim produced linewidths of $\Delta\nu_{1/2}(^1\mathrm{H}) \approx 7$ Hz for this setup.

3.4. Data processing

The first steps of post-processing were performed with the software LUISE (Siemens) of the MAGNETOM scanner: No k-space zero-filling, but a Hanning filter was applied prior to 2D FFT to the array of 8×8 spectra for damping the signal in the outer quarter of the matrix. In contrast, single FIDs were zero-filled to 4096 complex data points which corresponds to a frequency resolution of 0.038 ppm ≈1 Hz after FFT. Only one in vivo spectrum required exponential apodization (100 ms time constant); the other datasets were not line-broadened. Constant and different linear phase corrections were done on the scanner prior to transfer of the data to a PC for further post-processing with Origin 6.1 (OriginLab, Northampton, MA, USA). This included the baseline flattening tool and analysis of the spectra with the Levenberg–Marquardt algorithm assuming Lorentzian lineshapes of the resonances.

4. Results

From the 8×8 SI dataset covering both calfs, one voxel in the center of one calf was selected comprising

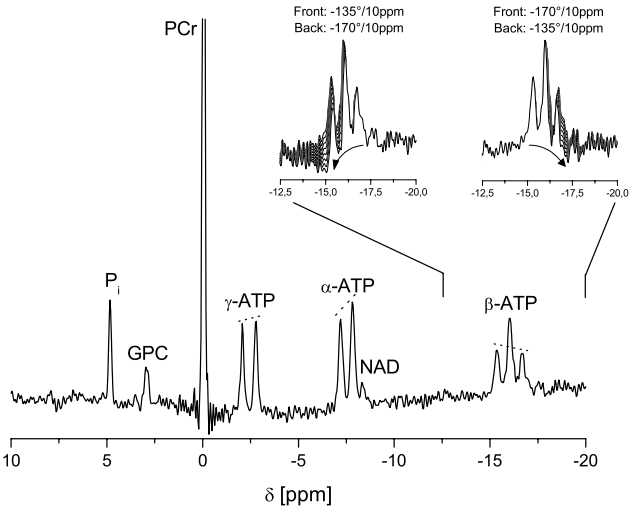

Fig. 3. In vivo $\{^1\mathrm{H}\}$–^{31}P NMR spectrum of the human calf illustrating the roof effect of the ATP multiplets (dashed lines). As a consequence of its large chemical shift, the β-ATP signal is quite sensitive to linear phasing. In this case, $\phi = -152°/10$ ppm is applied. Smaller $|\phi|$ cause a decreased and finally inverted roof effect of the β-ATP signal (upper left inset), larger $|\phi|$ exaggerate the effect (upper right inset). No baseline correction; experimental sequence parameters: SI with NOE signal enhancement and ^{1}H decoupling enabling resolution of the glycerophosphorylcholine (GPC) resonance, 8×8 voxels of size $31.25 \times 31.25 \times 50$ mm^3 each, $NEX = 20$, $TR = 1.1$ s, measurement time = 23.5 min.

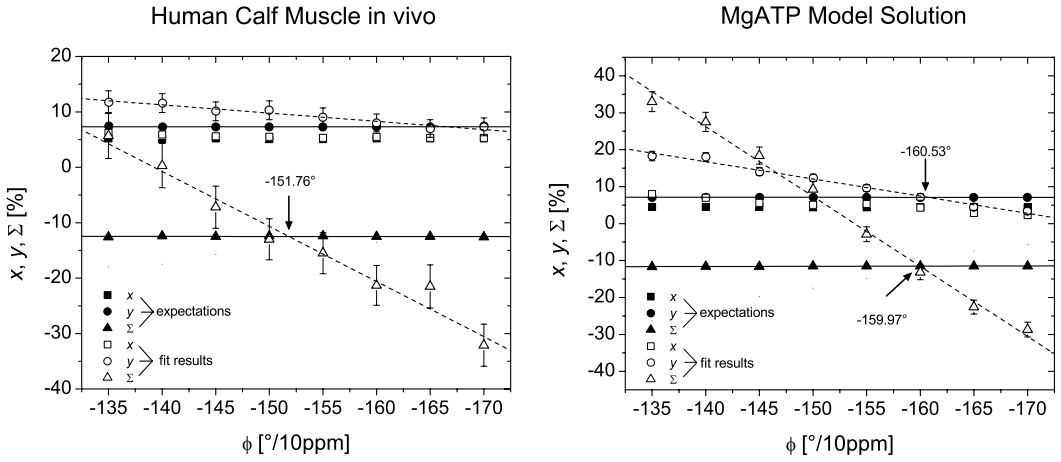

Fig. 4. Effect of different linear phasing ϕ on the corrections x, y, and Σ for data obtained in vivo and from an MgATP model solution (pH 7.03). Positive corrections represent an increasing (/), negative values a decreasing (\) "roof." The predictions (■, ●, ▲) derived from line positions and coupling constants are very stable. If the linear phasing is too small, the roof effect of the β-ATP resonance is inverted and that of the doublets exaggerated. Increasing the linear phasing, the fit results (□, ○, △) pass over the true value (intersection of solid and dashed lines). Because of partial overlap with the nicotinamide adenine dinucleotide (NAD, see Fig. 3) resonance, the effect for the β-ATP doublet in vivo is overestimated by the fit and the corresponding crossing is shifted to the right. In contrast, correct phasing of the resonances from model solutions can be obtained simultaneously (representative errorbars for fit results of y and Σ).

tissue both of m. soleus and m. gastrocnemius. The linear phase correction has a significant influence on the observable roof effect of the β-ATP resonance. This is demonstrated in Fig. 3. The effect is easy to identify for the two doublets, while its complement for the doublet-of-doublets is sometimes displayed incorrectly in the literature. An inadequate linear phase causes a cancelation or even an inversion of the effect for this resonance.

To determine the correct phasing ϕ, each spectrum was evaluated with eight different values $\phi = -135°$, $-140°, \ldots, -170°/10$ ppm (Fig. 4). These spectra were approximated by two Lorentzian doublets and one triplet comprising the variable parameters x, y, and Σ (an additional singlet was used to consider the composite signal of UDP glucose and nicotinamide adenine dinucleotides [NAD, NADH, NADP, and NADPH], in the following shortly NAD, on the high-field side of the α-ATP doublet). Because of the high resolution (the mean value for the linewidth of the β-ATP "triplet" components was (9.1 ± 2.4) Hz), the predictions for the roof effect derived from the line positions and coupling constants of each spectrum are very stable and can be used for accurate phase adjustment (Fig. 4): since the fit results for the correction parameters show a nearly linear dependence on the phasing, the true value of ϕ can be determined from the intersection of the linear fit of the Σ-values with the Σ-predictions. In principle, this method is also applicable to the corrections x and y, but the β-ATP multiplet enables the most reliable phasing for in vivo spectra (see Section 5).

Application of correct linear phasing was then followed by one fitting session in order to determine the actual line positions and $J_{i\beta}$ for final prediction of the correction parameters. χ^2 of a fit that considers the roof effect (with an accuracy of 10^{-3} for the correction parameters) was finally compared to χ^2 for an evaluation wit $x = y = \Sigma = 0$. All parameters for the different studies and mean values are listed in Table 1. The average improvement of the fits corresponds to a reduction

Table 1
Roof effect of ATP in in vivo ^{31}P NMR spectra of the human calf muscle at 1.5 T ($\omega_0 = 25.757$ MHz)

Study #	Linear phase (°/10 ppm)	$-\tan 2\vartheta_\gamma$ $(\frac{J_{\gamma\beta}}{\Delta\nu_{\gamma\beta}})$	$-\tan 2\vartheta_\alpha$ $(\frac{J_{\alpha\beta}}{\Delta\nu_{\alpha\beta}})$	x (%)	y (%)	Σ (%)	$\Delta\chi^2$ (%)
1	−145.78	$\frac{18.0(2)}{351.9(3)}$	$\frac{16.1(2)}{220.0(3)}$	5.11(6)	7.30(9)	12.42(11)	−3.0
2	−151.76	$\frac{18.1(1)}{350.8(1)}$	$\frac{16.2(1)}{219.6(1)}$	5.16(3)	7.34(4)	12.49(5)	−9.4
3	−160.72	$\frac{17.9(1)}{350.1(1)}$	$\frac{16.3(1)}{219.1(1)}$	5.10(4)	7.40(7)	12.50(8)	−10.8
4	−152.50	$\frac{19.4(2)}{352.1(2)}$	$\frac{16.5(2)}{220.1(2)}$	5.51(7)	7.47(9)	12.99(11)	−8.7
5	−156.87	$\frac{17.3(2)}{351.1(3)}$	$\frac{15.5(2)}{220.0(3)}$	4.92(6)	7.01(9)	11.93(11)	−11.1
Mean		$\frac{18.1(8)}{351.2(8)}$	$\frac{16.1(4)}{219.7(8)}$	5.16(22)	7.30(18)	12.46(37)	−8.6(3.3)

The mixing angles ϑ_γ and ϑ_α determine the correction terms x and y, respectively, and $\Sigma = x + y$. Accuracy of the correction parameters is high (last digits in brackets; 0.11% for Σ at most), so the interindividual variations dominate the uncertainty of the mean values (0.18–0.37%). Taking the roof effect into account improves all fits since χ^2 was reduced in each evaluation ($\Delta\chi^2$ column).

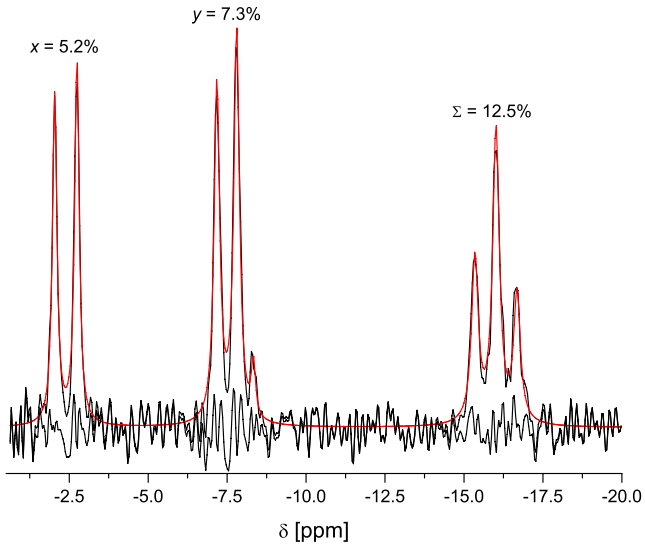

Fig. 5. In vivo ^{31}P NMR spectrum of ATP (and NAD) from human calf muscle (study # 2 of Table 1). The post-processed spectrum (black) after baseline and precise phase correction clearly exhibits the entire roof effect. For those high-resolution spectra (the linewidth of the β-ATP multiplet components is 6.6 Hz) accurate fitting of the post-processed data with Lorentzian lineshapes (red) requires the correction parameters x, y, and Σ; the difference signal (data − fit) is nearly noise. Experimental parameters, see Fig. 3.

of χ^2 by about 9% ($p < 0.005$ for a paired two-sample t test).

Fig. 5 demonstrates that the roof effect can be completely resolved in in vivo spectra after careful post-processing. Especially the doublet-of-doublets causes problems if the effect is ignored since three peaks violate the simple model of intensity ratios 1:2:1 and χ^2 increases mainly as a consequence of an inadequate approximation around $\delta \approx -16$ ppm.

For characterizing the average quantum-state mixing of the studied spin system in vivo, Table 2 displays the mean values of the mixing angles and CGCs. The mixing angles are small. Hence, breaking of the mutual spin–spin interaction by the external field is very effective, but first deviations from the Paschen–Back condition for the ^{31}P spin system in ATP can already be detected at 1.5 T.

^{31}P NMR spectra of ATP model solutions were recorded to explore whether the physiological parameters

Table 2
Mean values (and standard deviations) of quantum-mechanical state mixing of the ATP ^{31}P spin system in vivo at 1.5 T

Signal	δ (ppm)	Mixing angle (°)	CGC_1	CGC_2
γ-ATP	−2.37(2)	$\vartheta_\gamma = -1.48(6)$	0.99967(3)	−0.025(1)
α-ATP	−7.47(2)	$\vartheta_\alpha = -2.09(5)$	0.99933(3)	−0.0365(9)
β-ATP	−16.00(2)			

Note. $-\omega_0 = 25.757$ MHz; data from $n = 5$ volunteers. The Clebsch–Gordan coefficients are denoted $CGC_1 = \cos\vartheta$ and $CGC_2 = \sin\vartheta$. Accuracy of these coefficients is up to 3×10^{-5} (last digits in brackets).

[H^+] and [Mg^{2+}] have a measurable influence on this weak mixing of states. The line positions of ATP are susceptible to [H^+] in the range between pH 5 and pH 8 [10]. Although changes in chemical shifts of the three multiplets in vivo are mainly expected to originate from changes in Mg(II) chelation, we also studied the sole influence of pH variation on ATP spectra. The signal with the largest variance originates from the terminal ^{31}P nucleus (γ-ATP). It is clearly shifted to lower frequencies ($\delta = -2.79 \rightarrow -6.80$ ppm); the β-ATP resonance is shifted by 0.77 ppm in the same direction ($\delta = -18.45 \rightarrow -19.22$ ppm), while the shift of the α-ATP signal is less pronounced ($\delta = -7.70 \rightarrow -7.93$ ppm). Table 3 gives the corresponding parameters indicating that the roof effect of the γ-ATP doublet increases, while that of the α-ATP doublet slightly decreases upon acidification. The changes of Σ for the cumulative effect range within the limits of the uncertainty of the measurements.

To explore the effect of Mg(II) ions on the mixing of states in ATP, model solutions with equimolar amounts of $MgCl_2 \cdot 6H_2O$ and ATP were measured. The impact of complex formation is demonstrated in Fig. 6. A stronger shielding of the ^{31}P nuclei is induced, thus all resonances are shifted to higher frequencies. From the observation that the β-ATP multiplet undergoes the largest frequency shift ($\delta = -18.63 \rightarrow -16.38$ ppm) upon addition of Mg^{2+} ions to the neutral solution, the perturbation parameters are expected to increase. However, this effect is partially counteracted by the simultaneous decrease of the line splittings. A detailed analysis of x, y, and Σ is therefore needed, particularly in combination with data obtained from solutions with different pH.

In contrast to the signals of ATP, the resonances of MgATP only show changes for pH < 7 [10]. The corresponding results are found in Table 3. In neutral solution, the cumulative roof effect is reduced slightly compared to the pure ATP solution. Hence, the reduction of $J_{i\beta}$ by 3–4 Hz as a consequence of complex formation has a stronger effect on the state mixing than the decrease in $\Delta\nu_{i\beta}$. However, the reduction of Σ is very small (11.87% → 11.54%, Table 3). Altogether, the extreme values range within 11.48% (MgATP at pH 5.02) and 11.97% (ATP at pH 8). The average improvement of the fit as indicated by the reduction of χ^2 was $20.8 \pm 12.4\%$ ($p < 0.022$). In contrast to the in vivo experiments, the variance of $\Delta\chi^2$ is quite large.

Since small alterations of the ATP resonances in vivo are usually explained by changes in the intracellular Mg(II) concentration, we analyzed quantum-state mixing for the two neutral solutions (Table 4). The assumed increase of ϑ as a consequence of the pronounced downfield-shift of the β-ATP multiplet can hardly be observed for ϑ_α. Reduction of the coupling constants is more important and causes even a decrease of ϑ_γ upon ion

Table 3
Roof effect of ATP and MgATP in ^{31}P NMR spectra of model solutions at 1.5 T

Model solution Molecule (pH)	Linear phase (°/10 ppm)	$-\tan 2\vartheta_\gamma$ $(\frac{J_{\gamma\beta}}{\Delta\nu_{\gamma\beta}})$	$-\tan 2\vartheta_\alpha$ $(\frac{J_{\alpha\beta}}{\Delta\nu_{\alpha\beta}})$	x (%)	y (%)	Σ (%)	$\Delta\chi^2$ (%)
ATP (5.02)	−153.88	$\frac{18.5(3)}{320.0(2)}$	$\frac{18.0(5)}{276.7(3)}$	5.77(8)	6.06(16)	11.84(17)	−0.9
ATP (7.04)	−159.91	$\frac{19.1(1)}{388.5(1)}$	$\frac{19.2(1)}{274.7(1)}$	4.91(3)	6.96(4)	11.87(5)	−36.5
ATP (8.00)	−157.01	$\frac{19.6(2)}{403.3(2)}$	$\frac{19.3(2)}{271.0(2)}$	4.86(4)	7.11(6)	11.97(7)	−15.7
MgATP (4.00)	−161.98	$\frac{16.3(1)}{308.3(1)}$	$\frac{17.0(1)}{272.3(1)}$	5.29(2)	6.23(2)	11.52(3)	−20.1
MgATP (5.02)	−158.27	$\frac{15.8(4)}{330.8(4)}$	$\frac{16.7(4)}{248.5(4)}$	4.78(11)	6.70(14)	11.48(18)	−30.9
MgATP (7.03)	−159.97	$\frac{15.8(1)}{356.2(1)}$	$\frac{15.9(1)}{223.4(1)}$	4.44(3)	7.11(5)	11.54(5)	−20.7

The mixing angles ϑ_γ and ϑ_α determine the correction terms x and y, respectively, and $\Sigma = x + y$. Considering the roof effect reduces χ^2 (on average) by $20.8 \pm 12.4\%$ ($p < 0.022$). *Note.* $-\omega_0 = 25.758$ MHz, except for the experiment with ATP at pH 7.04 where $\omega_0 = 25.756$ MHz.

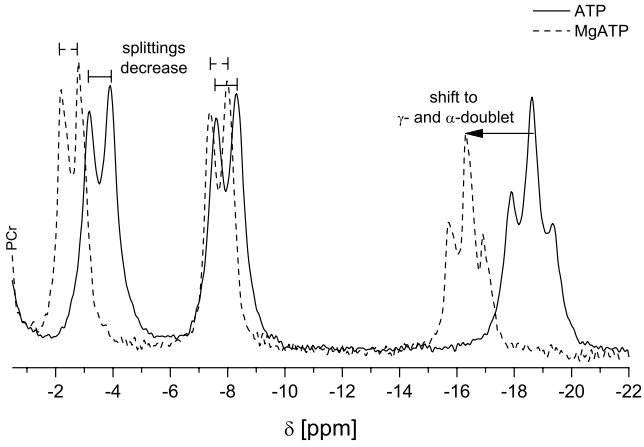

Fig. 6. ^{31}P NMR spectra of aqueous solutions of ATP (45 mM) and ATP with equimolar amount of Mg^{2+} at physiological pH (experimental parameters, see Fig. 3). Chemical shifts are relative to the PCr singlet at $\delta = 0$ ppm. The complex formation of the cation with the triphosphate chain diminishes the chemical-shift difference between the signal of β-ATP and its two coupling partners with the consequence of a stronger mixing of the eigenstates. This effect is partially counteracted by the simultaneous decrease of the line splittings.

chelation. Altogether, the CGCs derived from the in vivo spectra reflect a higher degree of state mixing than in the case of the neutral solutions. Concerning ϑ_α, spectra of all model solutions, irrespective of pH or complexation, yielded values smaller than those obtained from in vivo data. Only $\vartheta_\gamma = -1.6540(4)°$ for ATP at pH 5 was found to exceed the value of calf muscle tissue. Hence, the roof effect of the β-ATP multiplet as evaluated for m. gastrocnemius and m. soleus is supposed to represent the upper limit of observable successive state mixing.

5. Discussion

Phosphorus-31 NMR experiments on model solutions of ATP and the human calf muscle in vivo demonstrate that the complement of the roof effect of the α- and γ-ATP doublets can be identified in the β-ATP resonance. Careful post-processing of the FID reveals the true fine structure of the high-resolution spectrum even in vivo. Since the effect is less pronounced than in the case of the citrate signals in ^{1}H NMR spectroscopy, it suffices to approximate the cumulative intensity corrections in first order.

The derivation of Eqs. (2) and (3) in [4] yields single-quantum transitions with contributions from resonance frequencies of both nuclei. Neglect of the weaker contribution is permitted when the relative frequency differences are very small. This condition is fulfilled for the homonuclear ATP system, where the chemical-shift difference is less than 14 ppm in vivo.

Regarding a single spectrum, $J_{i\beta}$ and $\Delta\nu_{i\beta}$ can be determined precisely yielding reliable values x and y for the roof effect (accuracy of the order of 10^{-4}; x and y as independent fit parameters exhibit a 10 times larger standard deviation). Hence, interindividual variations are more important in vivo, but they are also known to be very small for these frequency-related parameters [7].

Table 4
Impact of complete complexation with Mg(II) ions on the quantum-mechanical state mixing of the ATP ^{31}P spin system at 1.5 T in neutral solution

Signal	δ (ppm)	Mixing angle (°)	CGC_1	CGC_2
γ-MgATP	−2.552(2)	$\vartheta_\gamma = -1.2712(3)$	0.999754(3)	−0.0222(1)
α-MgATP	−7.707(2)	$\vartheta_\alpha = -2.0379(5)$	0.999368(8)	−0.0356(2)
β-MgATP	−16.380(4)			
γ-ATP	−3.542(3)	$\vartheta_\gamma = -1.4082(3)$	0.999698(3)	−0.0246(1)
α-ATP	−7.959(3)	$\vartheta_\alpha = -1.9951(4)$	0.999394(7)	−0.0348(2)
β-ATP	−18.625(3)			

Accuracy of these single fits is higher compared to the mean values of in vivo data (Table 2). *Note.* $-\omega_0 = 25.756$ MHz for the experiment with MgATP; 25.758 MHz for that with ATP; pH 7.04 and 7.03, respectively. Nomenclature, see Table 2.

Evaluation of different linear phasings as demonstrated in Fig. 4 turned out to be appropriate to find the correct shape of the multiplets. Particularly useful is the β-resonance, which has the highest susceptibility of the ATP signals to linear phasing after adjusting the constant phase with the dominant PCr signal. Correct adjustment can be achieved simultaneously for the α-ATP doublet unless it overlaps partially with other signals (e.g., from NAD) which influence the response to different phasing. The γ-ATP signal should not be considered for this method since it might overlap with the intense PCr signal and linear phase corrections affect this doublet only to a minor degree because the chemical-shift difference is less than one-sixth compared to that of the β-ATP multiplet.

The spectral resolution of 1 Hz in our study is worse than tissue-specific variations of line positions in spectra of m. gastrocnemius and m. soleus reported by [12]. The indicated changes of the coupling constants in the two tissue types were at most 1 Hz for $J_{\gamma\beta}$—which is not important compared to our result $J_{\gamma\beta} = 18.1 \pm 0.8$ Hz. Therefore, tissue-specific variations within the calf concerning the roof effect of ATP at 1.5 T can be neglected.

Our study of five volunteers yielded values of x and y with an accuracy of about 2×10^{-3}. Evaluation of a larger group was found to be not necessary: since the roof effect is characterized by parameters derived from coupling constants and chemical shifts, we compared our data to results of previous in vivo studies where these quantities were determined with high accuracy (but which did not focus on this effect). For example, Jung et al. [7] obtained spectra of 13 volunteers and analysis of their data yields $x = 4.9(1)\%$, $y = 7.3(1)\%$, and $\Sigma = 12.2(2)\%$, which is quite consistent with our data (Table 1, bottom line).

The considerations of the cumulative roof effect of the β-ATP resonance are only valid if signal contributions of adenosine 5′-diphosphate (ADP) are insignificant. Otherwise the α- and γ-ATP doublets would contain signals which represent a connectivity by themselves. Since $J_{\alpha\beta}$ has nearly the same value in ADP and ATP, the roof effect of the two doublets would be more pronounced, because their $\Delta\nu$ is smaller than the frequency differences of the coupled resonances in the ATP spectrum. However, the activity of the ATP synthase shifts the equilibrium strongly to the triphosphate such that [ADP]:[ATP] ≈ 1:300 [13]. Contributions of other nucleoside di- and triphosphates can also be neglected [14]. Hence, the line intensities of the components of the two doublets are determined exclusively by the roof effect of ATP and the multiplet structure simulated in Fig. 1 is confirmed by the in vivo experiments.

The in vitro experiments showed that acidification causes a decrease in y and an increase in x for the ^{31}P resonances of ATP and MgATP (Fig. 7). Changes of x and y mutually compensate such that Σ is nearly independent of pH in both molecules.

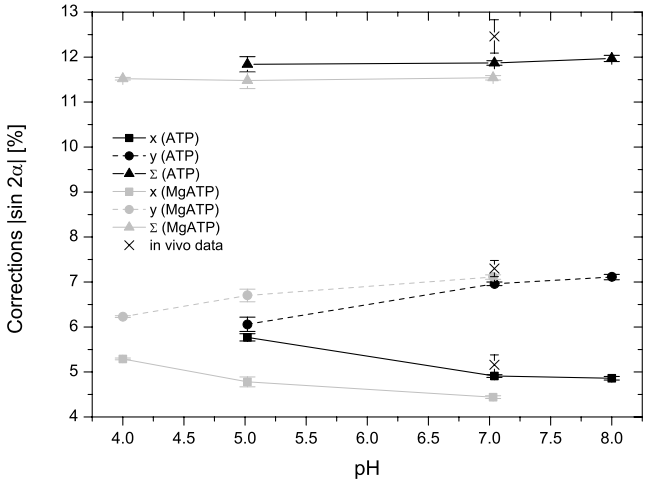

Fig. 7. Correction terms x, y, and Σ for ^{31}P NMR spectra of ATP and MgATP model solutions as a function of pH. Changes in x and y compensate mutually and yield a constant Σ. In the range of physiological pH, chelation of Mg(II) ions mainly induces changes in x, but barely in y. The mean values of in vivo experiments are also shown (×).

Previous studies showed maximum changes of ^{31}P chemical shifts and coupling constants in the case of $[Mg^{2+}]$:[ATP] ≈ 1, i.e., complete complexation of ATP [11,15] (this is consistent with the dissociation constant of the complex which reflects a high stability: 45 μM at 25 °C and 38 μM at 35 °C [16]). Hence the variations observed in our spectra represent the maximum effect of Mg^{2+}–ATP interaction on ATP spectra.

To consider (maximum) variation of intracellular $[Mg^{2+}]$, the degree of Mg(II) complexation in the physiological range of pH requires only a small modification of y in the range of $6.96 \leftrightarrow 7.11$; the effect of decreasing $J_{\alpha\beta}$ is slightly overcompensated by the reduction of $\Delta\nu_{\alpha\beta}$. A very high degree of complexation implies a reduction of $x = 4.91 \rightarrow 4.44$, which also reduces Σ since the similar shift of the γ- and β-resonances upon addition of Mg^{2+} cannot compensate the reduction of $J_{\gamma\beta}$. Because the observed coupling constant $J_{\gamma\beta}$ in vivo is distinctly larger than in neutral MgATP solution (18.1 Hz vs. 15.8 Hz), a strongly reduced J normally will not occur in vivo and a non-negligible fraction of ATP molecules in the cell is supposed to remain uncomplexed. Studies where $[Mg^{2+}]$ was determined from the chemical-shift difference of the α- and β-ATP signals indicate that ca. 90% of cellular ATP is complexed with Mg [12,16], but it is suspected that another mechanism partially compensates the effect of Mg(II) chelation on J [12]. Of course, only the resultant in vivo value of $J_{\gamma\beta}$—which is always larger than that of any MgATP model solution—accounts for the roof effect and is connected with the observed higher degree of state mixing in muscle tissue. If this value does not vary to such an extent that the mixing of the γ-ATP eigenstates is reduced, the parameter values $x \approx 5.2\%$ and $\Sigma \approx 12.5\%$ are well suited for fit of all in vivo spectra obtained at 1.5 T.

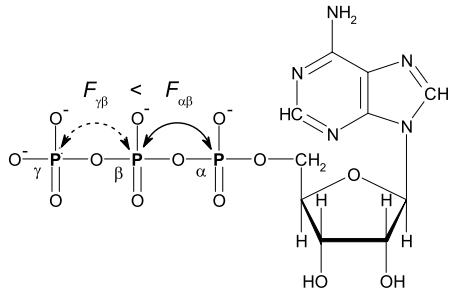

Fig. 8. The ATP molecule with the different remaining total ^{31}P spins F established by J coupling.

In contrast to the evaluation of in vivo spectra, the improvement of the fit of spectra of model solutions as expressed by the reduction of χ^2 shows a significant higher variance (Table 3). This is because spectra with large signal-to-noise ratio exhibit a small residual signal and hence small changes in χ^2 appear as relative large reductions. Moreover, this scattering produces a relative high p value. The ATP solution with pH 5.02 has a unique spectrum since the two doublets overlap such that a symmetric triplet appears. In this case, neglect of the roof effect could be compensated by modified amplitudes of the Lorentzian lineshapes and the improvement was poor. However, the mean value of $\Delta\chi^2$ demonstrates the improvement which is achieved by the consideration of the roof effect for both in vitro ($p < 0.022$) and in vivo ($p < 0.005$) spectra. Since the overall intensity of the multiplets is not affected by the roof effect, χ^2 is the adequate parameter to value the higher accuracy of the fit. Assuming symmetric multiplets will not falsify the quantification of the overall β-ATP intensity, but will miss the true lineshape.

The CGCs can be determined with high, although different accuracy. Interindividual variations again exceed the uncertainty of a single evaluation. Hence, the in vivo coefficients are less precise than those for the different model solutions. $CGC_2 = \sin\vartheta$, which quantifies the small admixture of the orthogonal eigenstate for increasing $|\vartheta|$, has a larger error because of the steep slope of the function at $\vartheta \approx 0$.

Regarding the CGCs of ATP obtained here, it is interesting to note that the remaining total spin is larger for the connectivity α–β although its coupling constant is smaller than $J_{\gamma\beta}$. This is a consequence of different $\Delta\nu$. According to Fig. 8 the shielding of the γ ^{31}P nucleus is stronger and yields a higher resonance frequency than for the α nucleus. The electrons affect the formation of the total spins F which results in $F_{\gamma\beta} < F_{\alpha\beta}$, although for the coupling constants $J_{\gamma\beta} > J_{\alpha\beta}$ is valid.

6. Conclusion

A cumulative roof effect caused by multiple J-couplings can be approximated by the sum of single interactions if the deviation from the Paschen–Back regime is small. The ^{31}P nuclei of ATP in a magnetic field with an inductivity of 1.5 T represent a system with such properties; the consequences can be observed in high-resolution in vivo spectra. Hence the simplification to symmetric AX doublets as it is often used for fitting routines is inadequate and this prior knowledge should be applied to the analysis of high-resolution in vivo NMR spectra in order to reduce χ^2 of the fits (about 9% in this study). The transition from Paschen–Back to Zeeman regime due to an "insufficient strong" field B_0 is characterized by CGCs that slightly modify the uncoupled base $|m_I, m_S\rangle$ and by a non-vanishing total spin. Experiments demonstrate that the mixing of states is very small, but definitely detectable, even in in vivo NMR.

Acknowledgments

The authors appreciate the support by Hans Gross, Siemens Medical Solutions, Erlangen, for providing outstanding performance of the scanner. Until they were forced in October 2004 to terminate operating the system, they could rely on an excellent equipment, particularly with respect to the homogeneity of the magnet. Critical, helpful comments by the referees are also acknowledged.

References

[1] F. Schick, H. Bongers, S. Kurz, W.-I. Jung, M. Pfeffer, O. Lutz, Localized proton MR spectroscopy of citrate in vitro and of the human prostate in vivo at 1.5 T, Magn. Reson. Med. 29 (1993) 38–43.
[2] R.R. Ernst, G. Bodenhausen, A. Wokaun, Principles of Nuclear Magnetic Resonance in One and Two Dimensions, Clarendon Press, Oxford, 1987.
[3] L. Schröder, C. Schmitz, P. Bachert, Phase modulation in dipolar-coupled A_2 spin systems: Effect of maximum state mixing in ^{1}H NMR in vivo, J. Magn. Reson. 171 (2004) 207–212.
[4] R.K. Harris, Nuclear Magnetic Resonance Spectroscopy, Longman Scientific and Technical, Essex, 1986.
[5] H. Friebolin, Basic One- and Two-Dimensional NMR Spectroscopy, Wiley-VCH, Weinheim, 1998.
[6] L. Schröder, P. Bachert, Evidence for a dipolar-coupled AM system in carnosine in human calf muscle from in vivo ^{1}H NMR spectroscopy, J. Magn. Reson. 164 (2003) 256–269.
[7] W.-I. Jung, S. Widmaier, U. Seeger, M. Bunse, A. Staubert, L. Sieverding, K. Straubinger, F. van Erckelens, F. Schick, G. Dietze, O. Lutz, Phosphorus J coupling constants of ATP in human myocardium and calf muscle, J. Magn. Reson. B 110 (1996) 39–46.
[8] P. Bachert, M. Bellemann, Kinetics of the in vivo ^{31}P–{^{1}H} nuclear Overhauser effect of the human calf muscle phosphocreatine resonance, J. Magn. Res. 100 (1992) 146–156.
[9] P. Bachert-Baumann, F. Ermark, H.-J. Zabel, R. Sauter, W. Semmler, W.J. Lorenz, In vivo nuclear Overhauser effect in ^{31}P–{^{1}H} double-resonance experiments in a 1.5-T whole-body MR system, Magn. Reson. Med. 15 (1990) 165–172.
[10] R.A. de Graaf, In Vivo NMR Spectroscopy: Principles and Techniques, Wiley, Chichester, 1998.

[11] T.-D. Son, M. Roux, M. Ellenberger, Interaction of Mg^{2+} ions with nucleoside triphosphates by phosphorus magnetic resonance spectroscopy, Nucleic Acids Res. 2 (7) (1975) 1101–1110.
[12] S. Widmaier, T. Hoess, W.-I. Jung, A. Staubert, G.F. Dietze, O. Lutz, ^{31}P NMR studies of human soleus and gastrocnemius show differences in the $J_{\gamma\beta}$ coupling constant of ATP and in intracellular free magnesium, MAGMA 4 (1996) 47–53.
[13] L. Stryer, Biochemie, Spektrum der Wissenschaft Verlagsgesellschaft, Heidelberg, 1990.
[14] A.L. Lehninger, Principles of Biochemistry, Worth Publishers, New York, 1982.
[15] F. Mitsumori, Phosphorus-31 nuclear magnetic resonance studies on intact erythrocytes. Determination of intracellular pH and time course changes in phosphorus metabolites, J. Biochem. 97 (1985) 1551–1560.
[16] R.K. Gupta, R.D. Moore, ^{31}P NMR studies of intracellular free Mg^{2+} in intact frog skeletal muscle, J. Biol. Chem. 255 (9) (1980) 3987–3993.